Pure Appl. Geophys. 167 (2010), 323–338

DOI 10.1007/s00024-009-0019-y

Pure and Applied Geophysics

# Integrated Geophysical and Morphotectonic Survey of the Impact of Ghab Extensional Tectonics on the Qastoon Dam, Northwestern Syria

J. Asfahani,[1] Y. Radwan,[1] and I. Layyous[1]

*Abstract*—The latent impact of the Ghab pull-apart basin tectonic setting and associated deformations resulting from active tectonics on the Qastoon Dam in northern Ghab in Syria have been evaluated. This was achieved by applying an appropriate methodology essentially based on morphotectonic mapping and integrated geophysical surveys consisting of electrical resistivity profiling, vertical electrical sounding and self-potential. The integrated interpretation of the acquired morphotectonic and geophysical data allowed the detection of subsurface deformed structures, either underlying the Qastoon Dam lake floor, or close to it. It is believed that these active structures were developed through the ongoing active tectonic processes occurring in the Northern Arabian plate. The tectonic survey proved that the N66.5°E striking Wadi Al Mashta fault, extending beneath the Qastoon Dam lake floor, is one of the youngest active structures, and that the intersection of the fault with the Qastoon Dam prism is a water-leaking point. Dam supporting measures, continuous monitoring and precautious disaster management are therefore recommended to be urgently adopted and practiced.

**Key words:** Qastoon and Zaizoon Dams, morphotectonic, integrated geophysical survey, active tectonics, Ghab, Syria.

## 1. Introduction

Zaizoon and Qastoon earth-filled dams, distanced 5 km apart at the northern parts of Ghab pull-apart basin, were constructed during 1990–1996 and set in operation in 1996. Zaizoon Dam collapsed in 2002, costing 20 lives, flooding 5 villages and submerging 8,000 ha of fertile agricultural land.

The severe consequences of this tragedy motivated the authors to conduct this research in order to evaluate the probable latent impact of the Ghab pull-apart basin tectonic setting as a whole, the N–S, NNE striking eastern Ghab faults and the associated deformation mapped at different sites at the eastern parts of Ghab pull-apart basin on the Qastoon Dam.

Previous studies showed that Syria lies at the northern margin of the Arabian plate, and to the south of the East Anatolian Fault (EAF) that separates the Arabian plate from the Anatolian plate. The N–S trending Dead Sea Fault System (DSFS), which crosses through the western parts of Syria and termed locally West Sham Fault System (WSFS), is a major sinistral transform plate boundary between the African (Levantine sub-plate) and the Arabian plates (Fig. 1). It accommodates their differential movement, linking the Red Sea/Gulf of Aqaba seafloor-spreading to Neo-Tethyan collision in Turkey, involving complex structural deformation controlled by the prevailing stress field along it. It is widely believed that a total 105 km sinistral motion has occurred on the DSFS southern segments to the south of the Lebanese restraining bend (Quennell, 1984; Beydoun, 1999). The sinistral motion on the system's northern segments is estimated as much as 20–25 km (Trifonov et al., 1991; Chaimov et al., 1990, 1992).

This difference between the two sinistral motions is explained by a double-episode lateral movement (e.g., Quennell, 1959) along it, accompanied by two phases of Red Sea opening. The first phase was expressed by a 60–65 km Miocene slip on the system's southern segment (Freund et al., 1970; Quennell, 1984). The Post-Miocene second phase was expressed by a 20 to 25 km sinistral motion on both system's southern and northern segments. This phase is accompanied by an additional 20 km suggested to be accommodated by shortening of the adjacent Palmyride fold and thrust belt (Chaimov

[1] Geology Department, Syrian Atomic Energy Commission, P.O. Box 6091, Damascus, Syria. E-mail: jasfahani@aec.org.sy

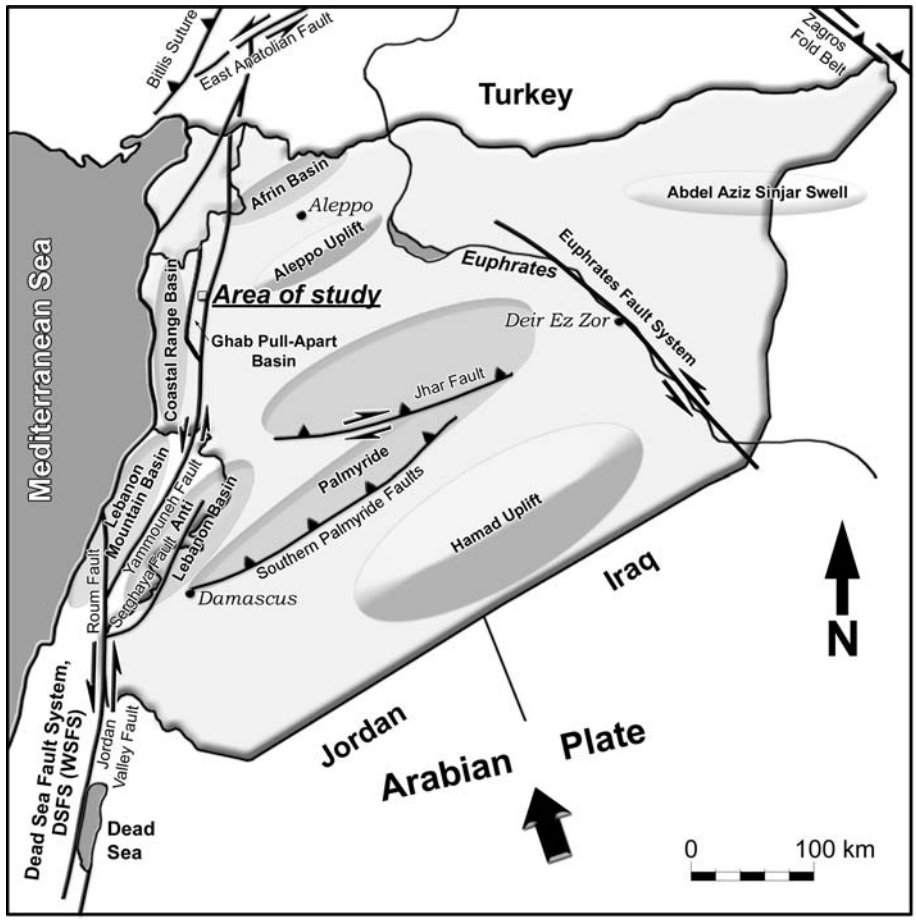


Figure 1
Major Structures in the Northern Arabian Plate

et al., 1990), making the total post-Miocene slip amounts 40–45 km, and 105 km on the northern system and southern segments, respectively.

However, Butler et al. (1997) argued that the northern segments of the DSFS (WSFS) have been inactive since the Miocene. Nevertheless, geomorphological evidence, for Pliocene-recent tectonic activity there, was reported by Hricko (1988), Darkal et al. (1990), Radwan et al. (1994a, b) and Devyatkin et al. (1997); Seismicity records (Ambraseys and Jackson, 1998); GPS measurements (McClusky and Balassanian, 2000; Gomez et al., 2006); paleoseismicity of Serghaya fault and Ghab pull-apart basin (Meghraoui et al., 2002, 2003; Gomez et al., 2001, 2003) attested to the current activity of the northern system segments. Radwan et al. (2004) restored tectonic and volcanic features on the eastern and western sides of Ghab pull-apart basin, and used them to estimate a 39-km sinistral movement on the system's northern segments of the DSFS.

The area of research is located around the Qastoon Dam, at the northeastern end of the 15-km wide and flat Ghab pull-apart basin, developed along the northern parts of the DSFS (WSFS) in Syria. Brew et al. (2001a, b) consider this pull-apart basin as a deep structure opened in response to a left-step in the DSFS during Pliocene to Holocene. It is bounded from the north and northeast by the NNE elongated Al Rouj Valley and Al Wastani Mountain. It is separated from Al Zawiyeh Mountain to the east and from the Coastal Chain to the west by bounding linear faults and to the south by a NW normal fault. The Ghab pull-apart basin is filled by horizontal,

90–150 m thick Pliocene lacustrine sediments, covered by a thin sheet of Quaternary lacustrine sediments (PONIKAROV, 1966).

The main objective of this research is to assess and clarify the impact of the tectonic setting of the Ghab pull-apart basin on the Qastoon Dam. This objective has been achieved by proposing and applying an appropriate methodology consisting of two approaches: namely, surface morphotectonic mapping and a multi-disciplined geophysical survey guided by the outcome of the morphotectonic mapping.

## 2. Geologic Setting

The area of research is located at the western rims of Jabal Al Zawiyeh, which overlooks Ghab pull-apart basin (Fig. 2). It is widely cultivated due to a favorable mild climate and moderate average rainfall (525 mm/y). The Qastoon Dam was constructed to catch surface runoff for irrigating plantations and orchards. Several wells were drilled in the research area, but unfortunately no borehole data are available. The outcropped 5–7° eastward dipping Cenomanian–Turonian sequence (150 m) consists of thin to moderately bedded limestone intercalated by (2–5 m-thick) marl intervals. The sequence is overlain by Campanian marl and limestone (40–45 m-thick). Two remarkable hiatuses were mentioned; the first lasted from Maestrichtian and ended with sedimentation of 180–225 m thick Middle and Upper Eocene marl, chalky limestone and limestone. The second hiatus lasted from Upper Oligocene and ended with sedimentation of 150-m thick Tortonian arenaceous marl, sandstone, clay, and conglomerate (PONIKAROV, 1966). Pliocene is dominated by 90–150 m thick lacustrine sediments, and deposited in a large lake that developed in the low areas represented by marl, clay, sandstone, and marl intercalated by thin levels of poorly preserved freshwater molluscs topped by algal limestone. Pliocene basaltic lava, tuff and scoria extruded from at least eight volcanic cones in the southern rims of the Al Wastani Mountain at the

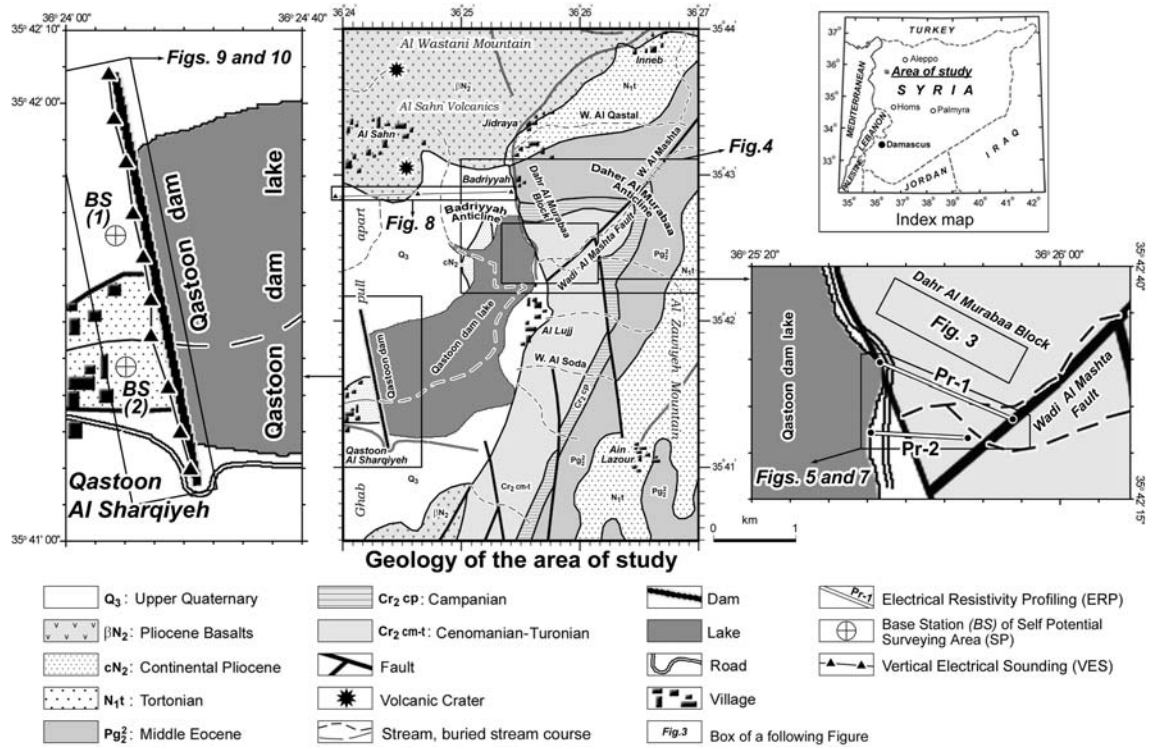


Figure 2
Geologic and tectonic map of Qastoon-Al Lujj area, northeastern Ghab pull-apart basin, northern Dead Sea fault system, northwestern Syria

intersection of Ghab pull-apart basin and Al Rouj valley near Jannaqra form a 2–60 m-thick basaltic cover (Ponikarov, 1966).

The Qastoon Dam is adjacent to the Dahr Al Murabaa block, which is a 2 by 4 km wedge-shaped block, extending between the villages of Jidraya, Badriyyah and Al Lujj. It is separated from Al Zawiyeh Mountain main block by a NE-striking sinistral strike-slip fault and bounded to the west by a NNW linear feature (Figs. 1 and 2).

Dahr Al Murabaa block layers are represented by moderately to thick bedded Cenomanian-Turonian limestone and dolostone, dip at 5–7° westward, overlain by Middle and Upper Eocene white massive limestone, Pliocene marly, chalky/clayey limestone and Quaternary clay, silt and marl. This rock sequence is faulted by *en echelon* set of 2.5–3-km long, 0.5–1 km spaced and 350° striking sinistral strike-slip faults (Fig. 2). Dahr Al Murabaa block is formed through the intersection of an 8-km long, 30° striking fault, i.e., Wadi Al Mashta sinistral strike-slip fault, and a NNW linear feature that extends from Al Lujj to Badriyyah, marking the northeastern shoreline of the Qastoon Dam lake. The Qastoon Dam lake is bordered from the north by Al Sahn basalt, extruded from two well-preserved volcanic cones in Pliocene (Fig. 2).

## 3. Methodology

The methodology proposed and applied in this research consists of performing the following consequent steps:

– Realizing surface morphotectonic mapping in Qastoon-Al Lujj area;
– Carrying out multi-disciplined geophysical survey guided by the morphotectonic mapping observations;
– Interpreting integratingly the measured geophysical data, which allow detection of new surface and subsurface small-scale structures, either adjacent to, or which underlie the Qastoon Dam lake floor;
– Evaluating the impact of the tectonic setting of the Ghab pull-apart basin and its potential danger to the Qastoon Dam.

### 3.1. Morphotectonic Mapping at Qastoon-Al Lujj Area

The field morphotectonic mapping established that the Dahr Al Murabaa wedge is actually an overturned anticline, with a 320° vergence termed by the authors "Al Lujj anticline". The anticline's southeastern limb is faulted by Wadi Al Mashta sinistral fault, while its northwestern limb is complicated by intensive deformation of its rock sequence (Fig. 3) as follows:

- Unit A: Normal faulting and folding of the lower unit;
- Unit B: Dip-slip faulting in the middle unit;
- Unit C: Sinistral strike-slip faulting in the upper unit.

Field mapping revealed also that the anticline's Eocene massive limestone top layers and the cN2 sediments, whose exposures extended farther north beyond the borders delineated by Ponikarov (1966), are deformed by similar folding, forming a core-faulted, N–S elongated double-plunging anticline (dip amounts 30° NW and SW), termed by the authors "Badriyyah anticline". The excavations for

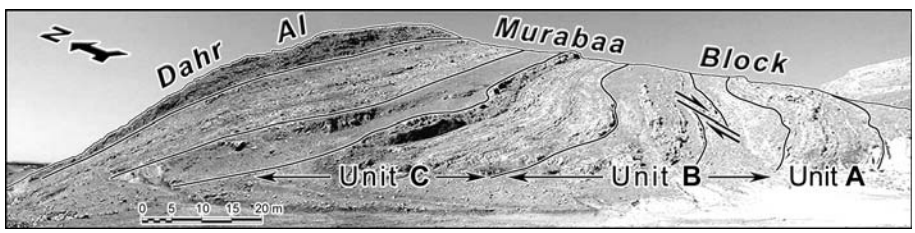


Figure 3
Faulting and folding of Dahr Al Murabaa block at Qastoon-Al Lujj area, looking northeast

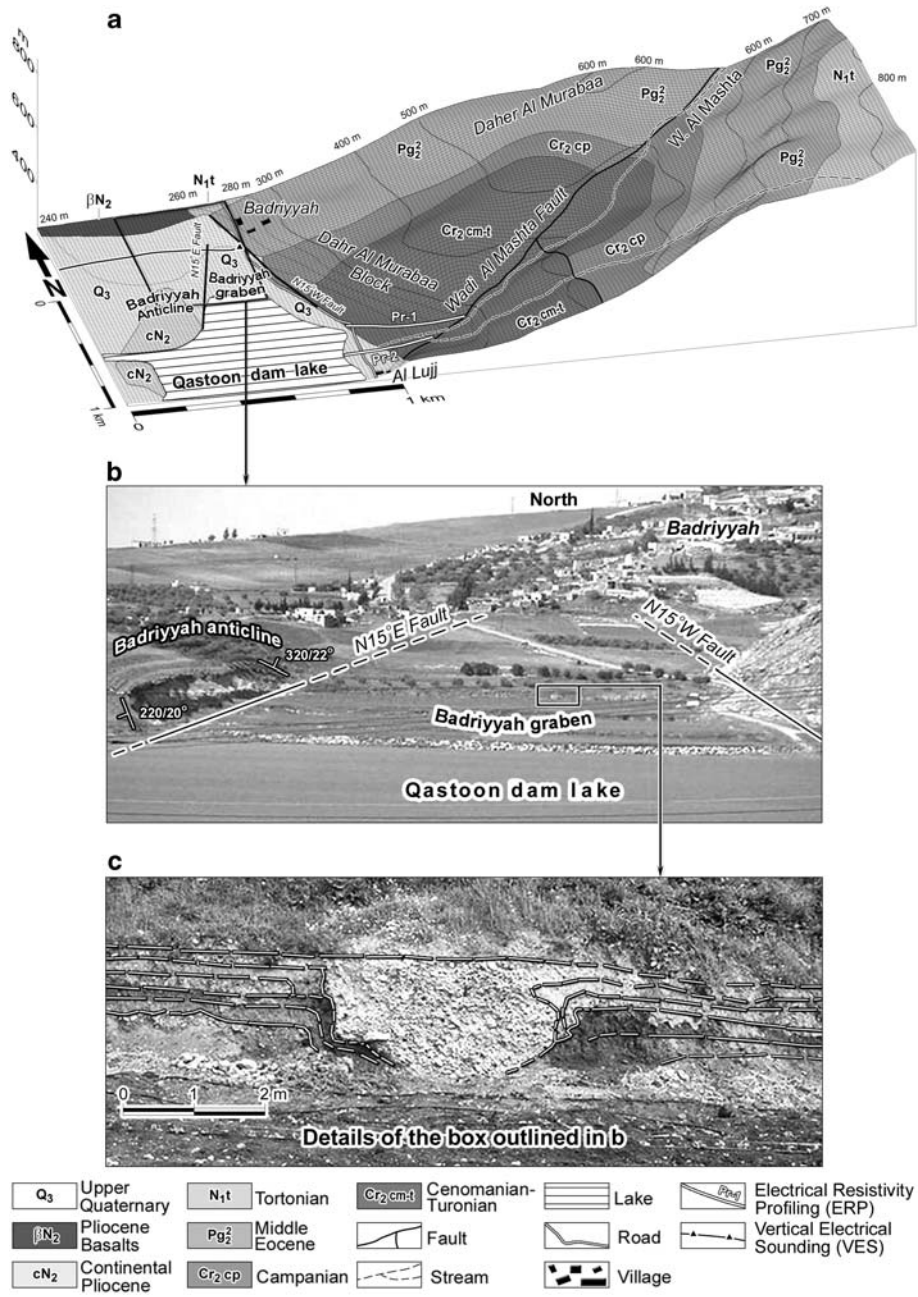


Figure 4
**a** A 3-D view dragged on the geological map. **b** Qastoon Dam lake and Badriyyah graben and anticline with a deep-cutting southward draining paleo channel. **c** Details of the mentioned channel buried by younger sediments

dam-filling material exposed a N15°E normal fault, which truncates the anticline's eastern flank (Fig. 4a, b). This fault represents the western boundary of a ~170 m narrow graben termed by the authors "Badriyyah graben". The eastern boundary of this graben is a N15°W striking normal fault which corresponds with the NNW linear feature that extends from Al Lujj to Badriyyah (Fig. 4a, b). The graben is filled by well sorted and graded Quaternary gravels, pebbles and very coarse sand beds, and faulted later

by 350° striking normal faults at its center, forming a less than 1-m wide superimposed graben. The course of a 60-cm deep paleo-channel draining southward to the low land, covered now by the Qastoon Dam lake water, was also mapped within the graben's sediments (Fig. 4b, c).

Such evidence suggests recent active vertical tectonics that started in the Early Quaternary and are ongoing, causing a steady subsidence of the central Badriyyah graben. The adjacent Qastoon Dam lake may be subject to the tectonic events.

### 3.2. Geophysical Survey

Various geophysical methods, such as electrical and electromagnetic profiling, electrical tomography,

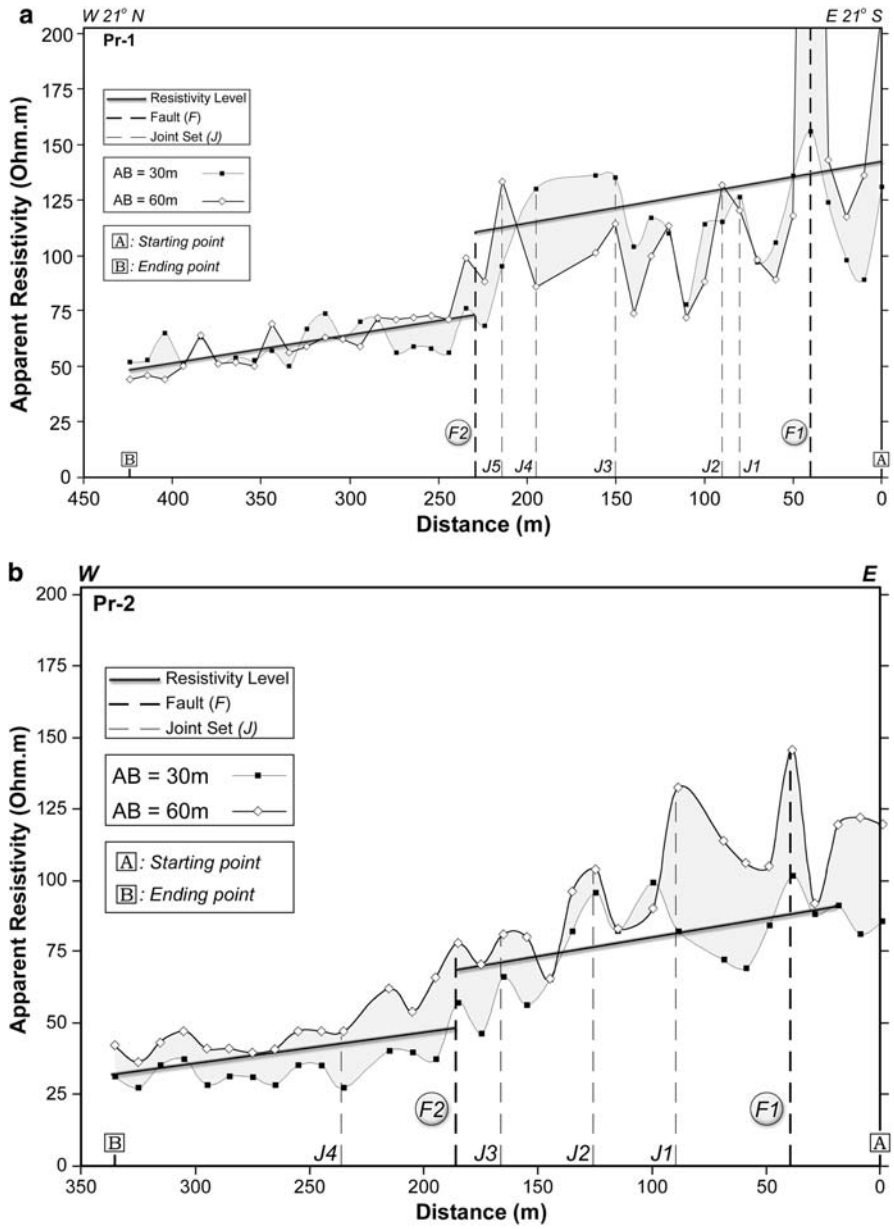


Figure 5
**a** Electrical Resistivity Profiling (ERP) along Pr-1 profile for two spacings of 30 and 60 m at Qastoon-Al Lujj area. **b** Electrical Resistivity Profiling (ERP) along Pr-2 profile for two spacings of 30 and 60 m at Qastoon-Al Lujj area

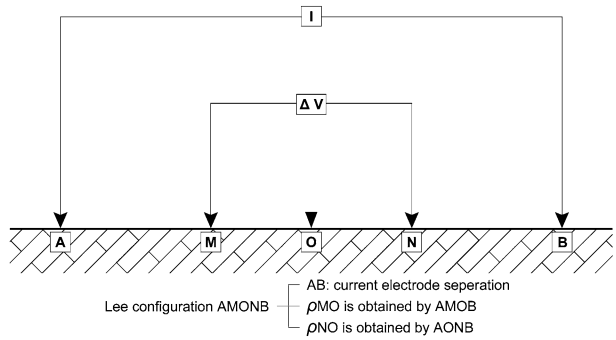


Figure 6
Lee configuration and its application in the field

refraction seismic, ground penetrating radar (GPR), high-resolution reflection seismic profiles can be used to image earth.

In this research, a DC geoelectrical survey was conducted in the Qastoon-Al Lujj area, using three different techniques: Electrical Resistivity Profiling (ERP); Vertical Electrical Sounding (VES); and self-potential (SP). Acquired measured data were interpreted in order to define the electrical characteristics of the penetrated rock formations, trace their lateral variations and to outline the tectonic subsurface image.

### *3.2.1 Electrical Resistivity Profiling (ERP)*

Using the ERP method, faults and fractures could be imaged and pinpointed at penetration depths ranging between 10 and 20 m. Electrical resistivity profiling was performed along two profiles at the Qastoon-Al Lujj site; the first one, labeled Pr-1, is 435-m long and oriented E21°S; the second one, labeled Pr-2, is 330-m long and E-W oriented (Figs. 2 and 4, 5a, b). Traditional Schlumberger configuration with two fixed AB constant spacings of 30 and 60 m (Figs. 2, 4 and 5a, b) was used for measuring the resistivity. A distance of 3 m between potential electrodes M and N was chosen. In fact, the choice of such current and potential spacings in this configuration has proven its efficacy in providing resistivity measurements from the required active tectonic depths. The computed geometric coefficients for AB of 30 and 60 m are 233 and 940 m, respectively. Forty points along the Pr-1 and thirty-two points along Pr-2 were measured with an interval of 10 m, between every two successive measurements.

Electrical resistivity profiling was also carried out using Lee configuration to detect the locations of the points of non-homogeneity, which could be interpreted and attributed to the presence of faults and fractures. This configuration includes the use of five electrodes AMONB placed on a straight line on the ground (where OM = ON), as shown in Fig. 6.

Three resistivities are measured by using such configuration as follows:

- Traditional $\rho$a results through A and B and measuring the potential difference between M and N;
- $\rho_{OM}$ resistivity results through electrical current between A and B and measuring the potential difference between M and O;
- $\rho_{ON}$ resistivity results through current between A and B and measuring the potential difference between N and O.

The geometric coefficients of Lee configuration are computed for current electrode AB spacings of 30 and 60 m to be 466 and 1880 m, respectively (the potential electrodes MN separation is constant and equals 3 m). The resistivity ratio variations $\rho_{OM}/\rho_{ON}$, for Pr-1 and Pr-2 profiles for both AB of 30 and 60 m, will be followed, traced and interpreted (Fig. 7a, b).

### *3.2.2 Vertical Electrical Sounding (VES)*

Vertical Electrical Sounding is generally used to determine vertical variations in electrical resistivity. In this technique, an electrical current is imposed by a pair of electrodes at a varying spacing expanding symmetrically from a central point, while measuring

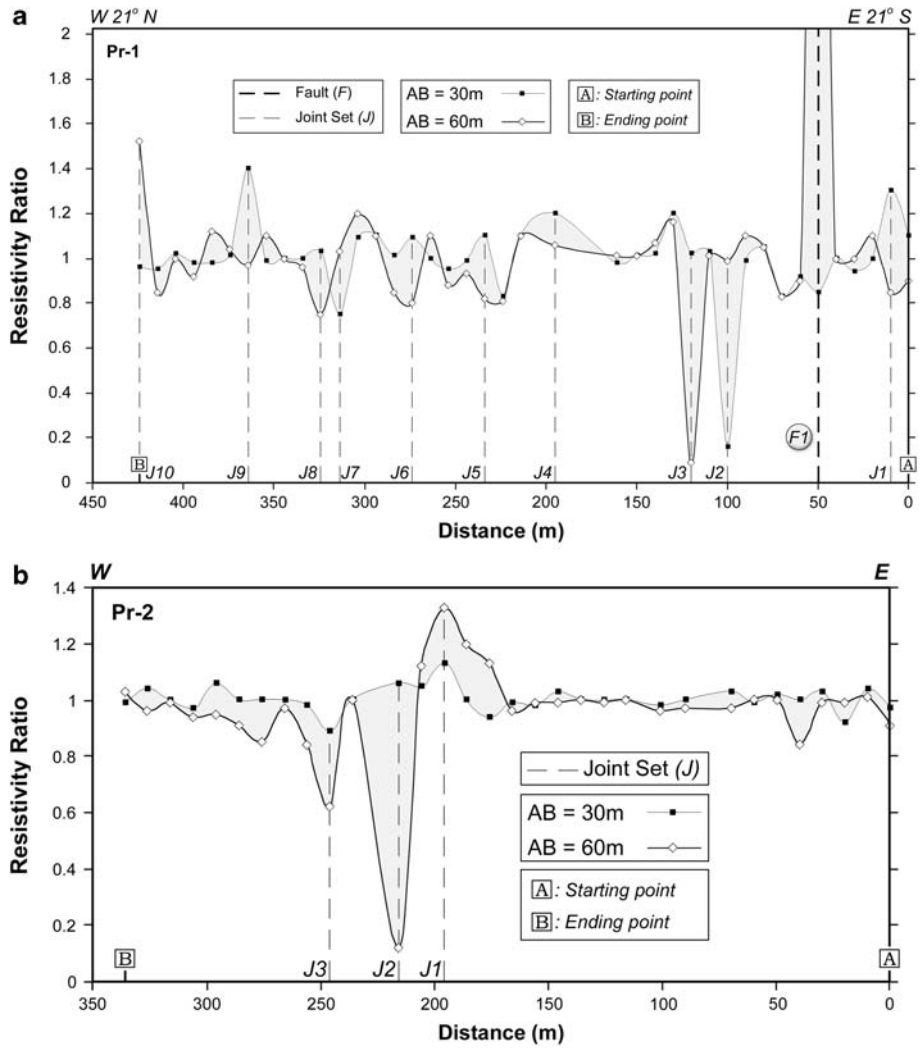


Figure 7
**a** Resistivity ratio along Pr-1 profile at Qastoon-Al Lujj area. **b** Resistivity ratio along Pr-2 profile at Qastoon-Al Lujj area

the resulting surface potential field with an additional pair of electrodes at appropriate spacing. For any array of current electrodes A and B and potential electrodes M and N, apparent resistivity $\rho$a is expressed according to Dobrin (1976) by:

$$\rho \mathrm{a} = K.\frac{\Delta V}{I}, \tag{1}$$

where

$$K = \frac{2\pi}{\frac{1}{\mathrm{AM}} - \frac{1}{\mathrm{BM}} - \frac{1}{\mathrm{AN}} + \frac{1}{\mathrm{BN}}}. \tag{2}$$

In the Eq. 1, $I$ is the current introduced into the earth and $\Delta V$ is the potential measured between the potential electrodes. The instrument used in this research measures directly the resistance $\frac{\Delta V}{I}$, and apparent resistivity $\rho$a is subsequently obtained after computing the geometric coefficient ($K$) for a given position of current and potential electrodes (Dobrin, 1976). Fine spacings were used in this research to detect shallow depth (<50 m) tectonic deformation in Quaternary sediments. In such shallow adapted configuration, the AB/2 spacing varies from 1 to 106.6 m, which allows a penetration depth of up to $\sim$50 m.

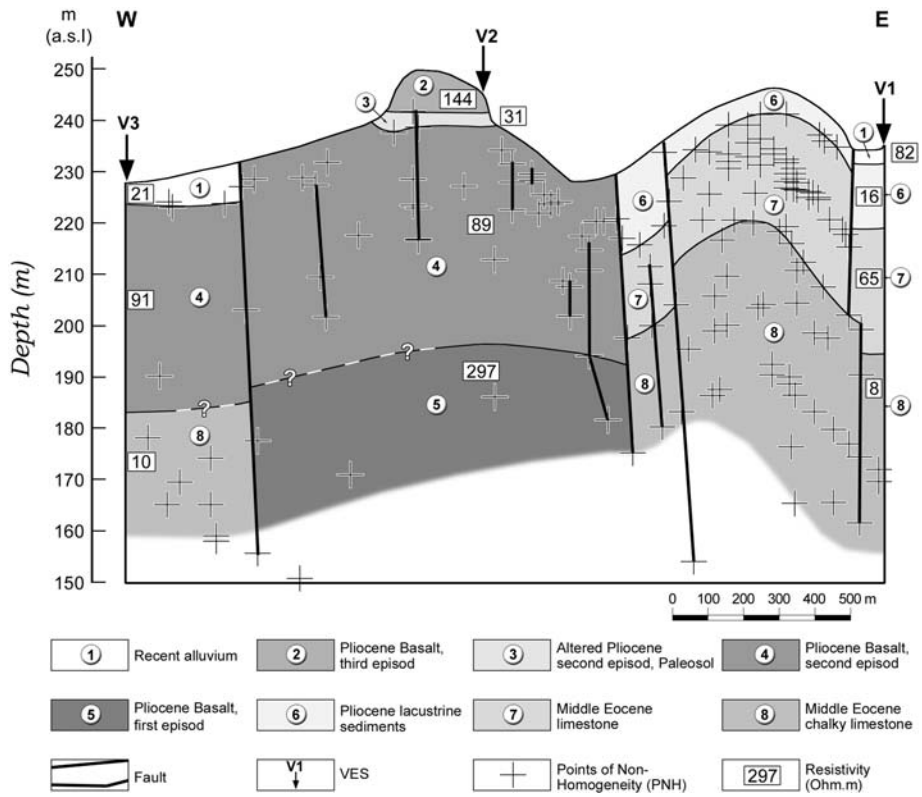


Figure 8
Shallow subsurface geoelectrical cross-section obtained along Badriyyah VES profile

An approximately ~3 km long, E-W oriented VES shallow geoelectrical profile was executed at the northern tips of the Qastoon Dam lake, perpendicular to the elongation of Badriyyah graben, detected through this research (Figs. 2, 8). And another geoelectrical VES profile, oriented NNW, 1750-m long, was executed parallel to the Qastoon Dam prism for shallow penetrations, in order to detect and locate points of tectonic weakness beneath the dam prism, as shown in Figs. 2 and 9.

### *3.2.3 Self-potential (SP)*

The self-potential method involves the measuring of the electric potentials at the surface. Such measured potentials are due to the electrochemical actions that can be developed in the earth by the contact between minerals and solutions. Using this technique, there is no need to impose an external electrical field on the earth. Measured SP current reaching more than 2 V can also be due to hydrological processes such as the electro-filtration phenomena. Such SP anomalies non-related to a sulfide-conductor and exceeding 2,000 mV were observed by LASFARGUES (1957) at Bas in Lower Congo. These observed elongated SP anomalies are attributed to water movement along a major fault associated with a brecciated zone.

The self-potential anomalies are detected by use of the nonpolarizing porous electrodes connected to the respective terminal of a milli-voltmeter. The potential differences are measured along profiles with pairs of such electrodes maintained at a fixed separation. Equipotential lines are obtained by maintaining one electrode at a base station (reference point), and moving the other electrode along the studied profile.

The SP method was applied at two fractured areas parallel to the Qastoon Dam (Fig. 9). This was carried out to trace and detect any water filtration and possible leakage from the dam lake (Fig. 10). At each area, an SP grid consisting of six N12°W striking profiles (Pr. A, B, C, D, E and F) and covering

approximately 126 m × 200 m at area 1, and 141 m × 200 m at area 2 was established, where 120 SP stations are measured in each grid, with an interval of 10 meters between every two successive measurements (Fig. 10).

## 4. Field Results and Discussion

### 4.1. Interpretation of (ERP) Measurements

The tectonically-oriented interpretation of ERP (Pr-1) indicates the presence of two different apparent resistivity regions traceable at both 10 and 20 m penetrating depths for AB of 30 m and 60 m respectively (Fig. 5a).

The first region extends 230 m westward from profile Pr-1, and is characterized by an average resistivity of ~130 Ohm m. Within this region, a sharp resistivity peak (more than 200 Ohm m) at 40 m from the profile starting at point A, was interpreted as a subvertical fault (F1). Less pronounced resistivity peaks were interpreted as possible parallel joint sets (J) (Table 1).

The second resistivity region extends from the 230 m point on the profile to the profile endpoint B, with a 60 Ohm m average resistivity. The deflection between these two resistivity levels was interpreted as another subvertical fault (F2). The weak resistivity peaks along this profile might be considered as minor deformational features.

Analysis of ERP (Pr-2) reveals a similar case, with two regions of average resistivities 75 and 40 Ohm m values (Fig. 5b). The slope between them is traceable at both 10 and 20 m penetrating depths

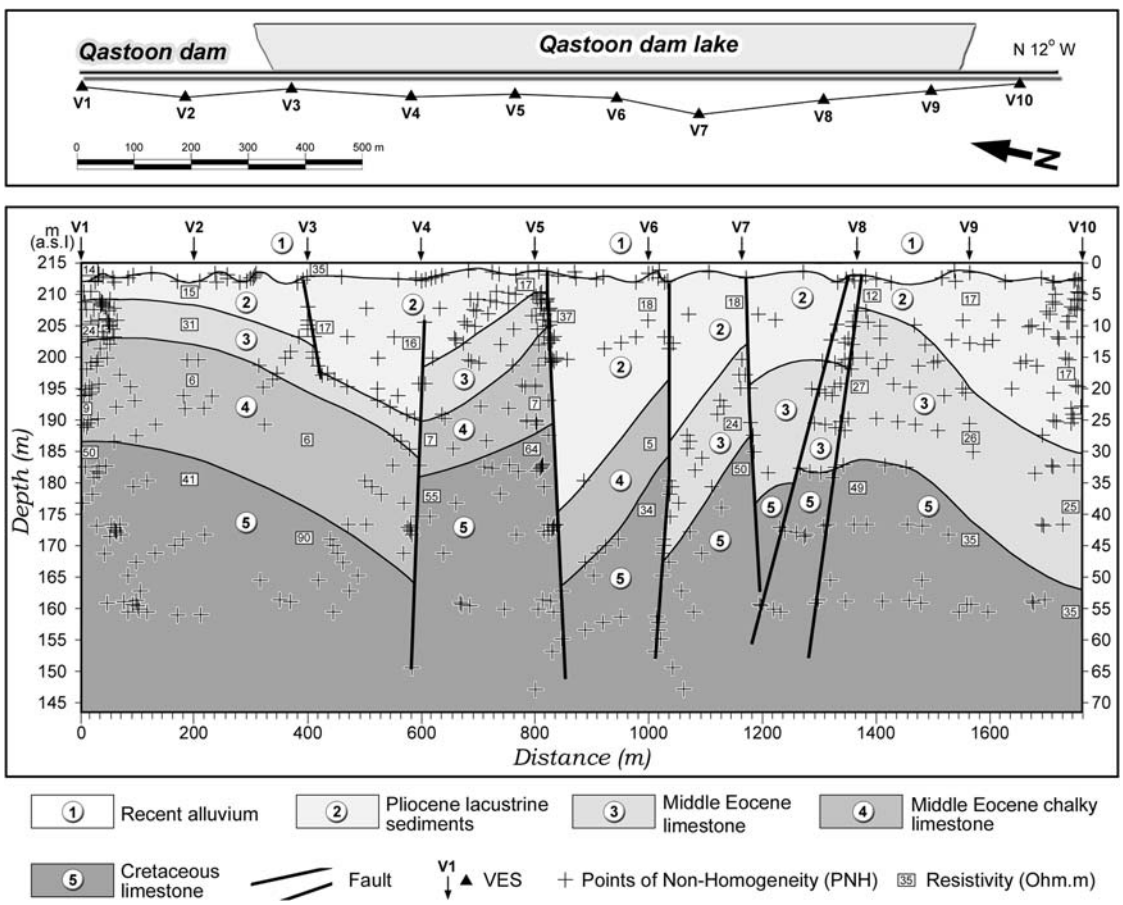


Figure 9
Shallow subsurface geoelectrical cross-section obtained along the Qastoon Dam VES profile

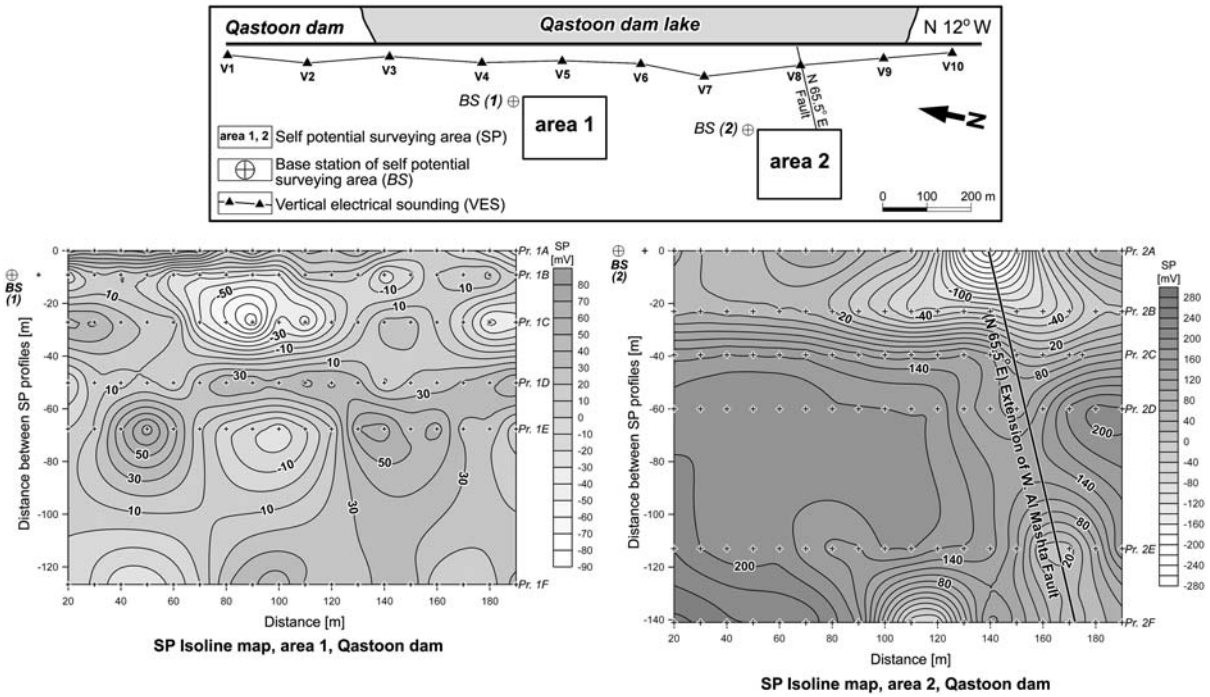


Figure 10
Self-potential isoline maps in areas 1 and 2 at the Qastoon Dam

Table 1

*Tectonic features detected on electrical resistivity profiling along E21°S Pr-1 and E-W Pr-2 at Qastoon-Al Lujj area*

| Distance of the peaks measured from the profile starting point A (m) | Resistivity [spacing AB (m)] | | | |
|---|---|---|---|---|
| | Pr-1 | | Pr-2 | |
| | 30 | 60 | 30 | 60 |
| 40 | F1 | F1 | F1 | F1 |
| 80 | J | | | |
| 90 | | J | | J |
| 125 | | | J | J |
| 150 | J | J | | |
| 165 | | | J | J |
| 185 | | | F2 | F2 |
| 195 | J | | | |
| 215 | | J | | |
| 230 | F2 | F2 | | |
| 235 | | | J | J |

*F* fault, *J* joint

for AB of 30 and 60 m respectively, marking a subvertical fault labeled (F2), distanced 185 m from the profile's starting point. A moderate peak is recognized in the 60 m-spaced AB, interpreted as (F1) fault distanced 40 m from the Pr-2 profile starting point. Less pronounced peaks were interpreted as joint sets (J) (Table 2).

F1 fault, traced on both profiles Pr-1 and Pr-2, was interpreted as the extension of the N66.5°E Wadi Al Mashta fault, while F2 fault was interpreted as a parallel fault to F1 (Fig. 5a, b).

### 4.2. *Interpretation of Resistivity Ratios Profiles (Lee Configuration)*

As a rule, resistivity ratio value of $\rho_{OM}/\rho_{ON} = \sim 1$, indicates an homogeneous medium between M and N electrodes. Ratio values deviating from 1 reflect a sharp geoelectrical contrast between adjacent media of different electrical characteristics, caused mainly by fractures and faults.

Ratio variations and characteristics of Pr-1 and Pr-2 profiles were shown in Fig. 7a, b and Table 2, respectively. They show values that differ from 1,

Table 2

*Tectonic features detected on resistivity ratio ($\rho_{OM}/\rho_{ON}$) along E21°S Pr-1 and E-W Pr-2 at Qastoon-Al Lujj area*

| Distance of the peaks measured from the profile starting point A (m) | Resistivity ratio [$\rho_{OM}/\rho_{ON}$ spacing AB (m)] | | | |
|---|---|---|---|---|
| | Pr-1 | | Pr-2 | |
| | 30 | 60 | 30 | 60 |
| 10 | J | | | |
| 50 | | F1 | | |
| 100 | J | | | |
| 120 | | J | | |
| 194 | J | | J | J |
| 220 | J | | J | |
| 246 | | | J | |
| 275 | J | | | |
| 316 | J | | | |
| 325 | | J | | |
| 365 | J | | | |
| 425 | | J | | |

*F* fault, *J* joint

interpreted accordingly as potential shallow active faults.

### 4.3. Interpretation of VES Profiles

Vertical resistivity soundings were interpreted by two approaches:

- The first interpretation approach is the curve-matching technique using master curves (Orellana and Mooney, 1966), giving approximate subsurface layers' thicknesses and resistivities. The approximate models were thereafter accurately interpreted using an inverse technique program (Zohdy, 1989; Zohdy and Bisdorf, 1989), until a good and reasonable fitness between field and regenerated theoretical curves is obtained.
- The second interpretation approach is based on the method of Pichgin and Habibullaev (1985).

This method is considered as the most sophisticated one for distinguishing tectonically fractured zones and oblique contacts between different rock types, and permits the determination of faults direction and dip amounts. When an electrical current passes through a plane contact between two outcropping formations of different resistivities $\rho 1$ and $\rho 2$, then electrical field boundary conditions at this contact are characterized by the following:

- If the center of vertical electrical sounding is exactly located over a vertical contact between two formations of different resistivities $\rho 1$, $\rho 2$, and the configuration is perpendicular to this contact, then the resulting measured resistivity $\rho$K is given by the following equation:

$$\rho K = (\rho 1 + \rho 2)/2 \tag{3}$$

and if the configuration is parallel to such a contact, then the resulting measured resistivity $\rho'$K is given by the following equation:

$$\rho' K = 2\,\rho 1\,\rho 2/(\rho 1 + \rho 2). \tag{4}$$

In both cases, the resistivity does not depend on AB or MN lengths.

- If there are two vertical electrical soundings VES1 and VES2, performed on either side of a vertical contact, then all profiling curves for every given AB/2 will be intersected in one point located over this vertical contact. The data of vertical electrical soundings are therefore converted to be represented by the form of horizontal curves as multi-depths profiling curves for every given AB/2. The locations of vertical electrical soundings, realized on a given profile, are plotted on abscissa using a linear scale, while the corresponding apparent resistivities ($\rho K$ or $\rho' K$) for each given AB/2 are plotted on ordinates using a logarithmic scale. The intersection points of all horizontal curves termed as "Points of Non-Homogeneity" (PNH), and labeled by (+) symbol are plotted on a 2-D ($x$, $z$) geological section. The depth $z$ of each of them can be determined according to the following equation:

$$Z = \left[(\mathrm{AB}/2)_i + (\mathrm{AB}/2)_j\right]/2 \tag{5}$$

where $(\mathrm{AB}/2)_i$ and $(\mathrm{AB}/2)_j$ are the half separations between the electrodes A and B, for which two horizontal curves are intersected. The fractured zones are

identified and determined by the presence of (PNH) on vertical pseudo-vertical lines.

The geological interpretation of the PNH is based on the following assumptions:

- When the (PNH) are distributed according to the oblique lines located at shallow depths, they point to the presence of an inhomogeneous lithological contact;
- If they are arranged along oblique lines dipping down at an angle exceeding 30° in depth, they represent a tectonic fractured zone;
- If they are randomly scattered near the surface, they indicate an homogeneous lithology;
- If they are arranged in a regular form, their reflection may be the presence of geological structures in the region of study (syncline, anticline, or simply horizontally layered strata).

More recently, ASFAHANI and RADWAN (2007) enhanced the method by taking into consideration the real topographic variations of the studied soundings (VES) distributed along a given profile, in order to accurately acquire reliable subsurface structures.

### 4.4. Interpretation of Badriyyah VES Profile

The interpretation of the VES by the inverse modeling revealed the presence of a lithological sequence that contains Middle Eocene chalky limestone and limestone, followed by Pliocene lacustrine marl and chalky limestone, caped by Pliocene basaltic flows and ending up by Quaternary alluvial sediments. By comparison, the interpretation of the same VES profile by the Pichgin and Habibullaev method shows a clear deformation represented by faulting and folding of the previously mentioned sediments, where these results are in accordance with surface morphotectonic mapping. Integration of the results suggests the presence of a vertical, ~50-m deep normal fault, defining the western side of the 170-m wide Badriyyah grabens. This finding is confirmed by the morphotectonic surface mapping of two normal faults striking N15°W and N15°E (Fig. 4a, b). Folding of the Eocene and Pliocene sediments, confined between the Badriyyah graben's western fault and Al Sahn volcanics, have been observed through the interpretation of VES data. The interpretation findings were in concordance with surface morphotectonic field mapping that yields to detect the Badriyyah anticline (Fig. 8). The geoelectrical interpretation also detected faults that bound and penetrated Al Sahn basaltic volcanics, erupted in Pliocene and Holocene, due to active tectonic processes.

The geoelectrical interpretation of Badriyyah VES profile confirms the presence of meaningful active tectonic deformation. The Badriyyah anticline and graben, folding and normal faulting of Pliocene sediments and normal faulting of Quaternary sediments which fill the aforesaid graben are evident examples of such deformation (Fig. 8). A southward draining paleo channel incising through them (Figs. 4b, c), and the presence of younger sediments burying this channel point to ongoing tectonics reflected by late steady subsidence of Badriyyah graben's central part, making it a potential water leakage site from the Qastoon Dam lake.

### 4.5. Interpretation of the Qastoon Dam VES Profile

The interpretation of the N12°W shallow VES profile of 1,750 m long, which measured parallel to the Qastoon Dam, allowed the obtaining of a geoelectrical subsurface image beneath the dam prism (Fig. 9). It defined three pronounced spots with clear alignments of the Points of Non-Homogeneity (PNH) beneath V1, V5 and V8 soundings. The (PNH) alignment beneath V1 is relatively less significant since it lies beneath the dam's northern end. The other two PNH alignments under V5 and V8 are alarming since they underlie the central part of the Qastoon Dam prism. They have been interpreted by considering the distribution of the measured resistivities values, as a SW extension of the NE-striking Wadi Al Mashta fault. Accordingly, V5 and V8 sites were selected to conduct SP measurements for detecting any possible water leakage at them from the dam lake.

### 4.6. Interpretation of Self-potential Surveying

In this connection, it is worth mentioning that after the Zaizoon Dam collapse, the Qastoon Dam Monitoring Authority installed 18 geodetic monitoring points on the dam prism and another 15 points at

the dam's backside, to monitor land deformation in the area surrounding the dam. The Authority also conducts continuous leveling using three- primary fixed benchmarks, seven secondary benchmarks and eight roving ones. The Qastoon Dam water-controlling team, responsible for monitoring lake water level, spotted three water-leaking points. The first one is situated at the dam prism; the second one is located at the basaltic rocks that outcrop at the dam lake northern bank, while the third is located 200 m west of the dam. These observations are important, particularly the presence of the second leaking point, since it coincides with the N15°E striking normal fault that defines the western border of the above-mentioned Badriyyah graben. The first leaking point will be discussed in the following paragraph.

Two SP grids were established over areas 1 and 2, where the locations of V5 and V8 are respectively covered (Fig. 10). The map of SP for area 2 clearly reveals a N65°E SP elongated anomaly. The elongation axe is distanced 325 m from the southern end of the dam prism, and indicates a possible water leakage from the Qastoon Dam along it.

Remarkably, this elongation coincides with the direction of the NE-striking Wadi Al Mashta fault. This strengthens the interpretation of a southwestern extension of the Wadi Al Mashta fault beneath the dam lake's floor and the dam itself (Figs. 2, 10). Croos-cut relationships indicate that the Wadi Al Mashta fault is either younger than the N15°W fault, which bounds the Badriyyah graben's eastern end, or it is an older fault that underwent a later reactivation. Accordingly, Wadi Al Mashta fault's formation and/or reactivation is indeed very recent, and its future reactivation with quite probably represent a real adjourned danger on the Qastoon Dam.

The map of SP established in area 1 could be interpreted as shallow jointing set conjugate to the Wadi Al Mashta fault (Fig. 10). The presence of 10° and 20° dipping Pliocene marly clay, clayey marl and clay horizons, forming the limbs of Badriyyah anticline, are hazardously lubricant horizons able to trigger slumping within the Qastoon Dam lake in response to a probable future earthquake. This bears an additional latent danger pending on the Qastoon Dam itself and on the surrounding villages.

## 5. Conclusion

The probable latent impact of the Ghab pull-apart basin tectonic setting at the northern segment of the DSFS (WSFS) in Syria and the associated active tectonic deformations on the Qastoon Dam have been evaluated.

An appropriate methodology consisting mainly of surface morphotectonic mapping and a multi-disciplined geophysical survey has been proposed and applied in this research. This methodology proved its efficacy through the following points:

- The morphotectonic mapping unveiled the presence of small-scale active tectonic structures, which are very close to the Qastoon Dam in northeastern Ghab pull- apart basin;
- The geophysical surveying carried out in this research is thematically oriented and guided by the tectonic mapping findings;
- The newly adapted shallow depth VES configuration with a penetration depth of approximately 50 m proved its superiority and advantage through the detection of faulting and folding at shallow depths (up to 50 m) i.e., Quaternary deposits, and the hidden subsurface tectonic structures.

Integration of results allows the detection of important structures, such as the Badriyyah anticline and graben, their bounding faults and the Wadi Al Mashta fault. These structures are believed to be the expressions of ongoing active tectonic processes. The proximity of such active structures to the Qastoon Dam lake represents a potential threat. It is therefore recommended to run continuous alarming monitoring procedures and adopt precautious disaster management measures in order to overcome any probable misfortune.

The proposed methodology has been successfully applied on the Qastoon Dam as a case study in Syria, and therefore can be applied on other dam locations suffering from leakage problems. This methodology is also recommended to be strongly applied in and around any area selected for construction of a future dam to evaluate the location validity.

*Acknowledgment*

The authors would like to thank Dr. I. Othman, Director General of the Atomic Energy Commission of Syria (AECS) for his permission to publish this paper. Professor Graham Heinson, editor of Pure and Applied Geophysics from the Adelaide University—Australia is deeply thanked for his critics and editing corrections. The two anonymous reviewers are also thanked for their comments and suggestions which considerably enhanced the paper.

## References

Ambraseys, N.N. and Jackson, J.A. (1998), *Faulting associated with historical and recent earthquakes in the Eastern Mediterranean Region*, Geophys. J. Internat. *133*, 390–406.

Asfahani, J. and Radwan, Y. (2007), *Tectonic evolution and hydrogeological characteristics of Khanaser Valley, Northern Syria, derived from the interpretation of vertical electrical soundings*, Pure Appl. Geophys. *164*, 2291–2311.

Beydoun, Z.R. (1999), *Evolution and Development of the Levant (Dead Sea Rift) Transform System: A historical–chronological review of a structural controversy*. In (MacNiocaill C, Ryan P.D., eds.), *Continental Tectonics*, J. Geolog. Soc. *164*, 239–255.

Brew, G., Barazangi, M., Al-Maleh, K., and Sawaf, T. (2001a), *Tectonic and Geologic Evolution of Syria*, GeoArabia *6*(3), 573–616.

Brew, G., Lupa, J., Barazangi, M., Sawaf, T., Al-Imam, A., and Zaza, T. (2001b), Structure and tectonic development of Al-Ghab basin and the Dead Sea fault system, Syria, J. Geolog. Soc. *158*, 665–674.

Butler, R.W.H., Spencer, S., and Griefeth, H.M. (1997), *Transcurrent fault activity on the Dead Sea transform in Lebanon and its implications for plate tectonics and seismic hazard*, J. Geolog. Soc. *154*, 757–760.

Chaimov, T., Barazangi, M., Al-Saad, D., Sawaf, T., and Gebran, A. (1990), *Crustal shortening in the Palmyride fold belt, Syria, and implications of movement along the Dead Sea fault system*, Tectonics *9*, 1369–1386.

Chaimov, T., Barazangi, M., Al-Saad, D., Sawaf, T., and Gebran, A. (1992), *Mesozoic and Cenozoic deformation inferred from seismic stratigraphy in the southwestern intracontinental Palmyride fold-thrust belt, Syria*, Geolog. Soc. Am. Bull. *104*, 704–715.

Darkal, A.N., Krauss, M., and Ruske, R. (1990), *The Levant fault zone: An outline of its structure, evolution and regional relationships*, Z. Geol. Wiss. Berlin *186*, 549–562.

Devyatkin, E.V., Dodonov, A.E., Sharkov, E.V., Zykin, V.S., Simakova, A.N., Khatib, K., and Nseir, H. (1997), *The El-Ghab Rift depression in Syria: Its structure, stratigraphy and history of development*, Stratig. Geolog. Correlation *5*(4), 362–374.

Dobrin, M. *Introduction to Geophysical Prospecting* (Mc Graw-Hill, New York 1976).

Freund, R., Garfunkel, I.Z., Goldberg, M., Weissbrod, T., and Derin, B. (1970), *The shear along the Dead Sea rift*, Phil. Trans. R. Soc. of Lond., A *267*, 107–130.

Gomez, F., Meghraoui, M., Darkal, A.N., Sbeinati, R., Darawcheh, R., Tabet, C., Khawlie, M., Charabe, M., Khair, K., and Barazangi, M. (2001), *Coseismic displacements along the Serghaya fault: An active branch of the Dead Sea fault system in Syria and Lebanon*, J. Geolog. Soc. *158*, 405–408.

Gomez, F., Meghraoui, M., Darkal, A.N., Hijazi, F., Mouty, M., Suleiman, Y., Sbeinati, R., Darawcheh, R., Al-Ghazzi, R., and Barazangi, M. (2003), *Holocene faulting and earthquake recurrence along the Serghaya Branch of the Dead Sea Fault system in Syria and Lebanon*, Geophys. J. Internat. *153*(3), 658–674.

Gomez, F., Khawlie, M., Tabet, C., Darkal, A.N., Khair, K., and Barazangi, M. (2006), *Late Cenozoic uplift along the Northern Dead Sea Transform in Lebanon and Syria*, Earth Planet. Sci. Lett. *241*, 913–931.

Hricko, J. (1988), *Geophysical exploration in selected areas of Syrian Arab Republic: Stage report on survey in Jisr Al Shoghour Area*, Unpublished internal report Strojexport Praha—Geofysika Brno, Czechoslovakia, Damascus/Brno.

Lasfargues, P. (ed.) (1957), *Prospection Electrique par Courants Continues*, Masson and C$^{ie,}$, 120 Boulevard Sain Germain, Paris (VI).

McClusky, S. and Balassanian, S. (2000), *GPS constraints on plate Kinematics and dynamics in the Eastern Mediterranean and Caucasus*, J. Geophys. Study *105*, 5695–5719.

Meghraoui, M., Gomez, F., Sbeinati, R., Van der Woerd, J., Mouty, M., Hijazi, F., Darkal, A.N., Darawcheh, R., Radwan, Y., Al Najjar, H., Layyous, I., Al Ghazzi, R., and Barazangi, M. (2002), *Late Holocene Paleoseismic Timing and Slip History along the Missyaf Segment of the Dead Sea Fault in Syria, Workshop on Environmental Catastrophes and Recoveries in the Holocene*, Brunel University Uxbridge, UK, August 29–September 2.

Meghraoui, M., Gomez, F., Sbeinati, R., Van der Woerd, J., Mouty, M., Darkal, A.N., Radwan, Y., Layyous, I., Al Najjar, H., Darawcheh, R., Hijazi, F., Al Ghazzi, R., and Barazangi, M. (2003), *Evidence for 830 years of seismic quiescence from palaeoseismology, archaeoseismology and historical seismicity along the Dead Sea fault in Syria*, Earth Planet. Sci. Lett. *210*, 35–52.

Orellana, E. and Mooney, H.M. (1966), *Master tables and curves for vertical electrical sounding over layered structures*, Interciencia, Madrid.

Pichgin, N.I. and Habibullaev, I.K.H. (1985), *Methodological recommendations in studying geo-tectonic conditions of vertical electrical soundings data with application of EC computer for solving hydrogeological and geo-Engineering Problems*, Tashkend (in Russian).

Ponikarov, V.P. (ed.) (1966), *The Geological Map of Syria*, scale 1:200000, sheets I-37-XIX and I-36-XXIV, Ministry of Industry, Damascus.

Quennell, A.M. (1959), *Tectonic of the Dead Sea Rift*, Proc. 20th Internat. Geolog. Congress, Mexico, 385–403.

Quennell, A.M. (1984), *The Western Arabia Rift System*. In (Dixon J.E., Robertson A.H.F., eds.), *The Geological Evolution of the Eastern Mediterranean*, J. Geolog. Soc. *17*, 775–788, Special publications.

RADWAN, Y., NAJJAR, H., and LAYYOUS, I. (1994a), *Indications of neotectonics along the Syrian Lebanese fault* (*AL-Ghab depression*), Proc. Regional Workshop on Archaeological Seismicity in the Mediterranean Region, Atomic Energy Commission of Syria, Damascus, 4–7 Nov. 1992, 122–133.

RADWAN, Y., NAJJAR, H., and LAYYOUS, I. (1994b), *Investigations of active tectonic along the major faults in Syria using geomorphic techniques*, Proc. Second Internat. Conf. *Geology of the Arab World*, Cairo University, 22–26 Jan. 1994, *II*, 59–71.

RADWAN, Y., NAJJAR, H., LAYYOUS, I., and RAMMAH, S. (2004), *Study of neotectonic features in Pliocene and Quaternary deposits along the Syrian Coast*, Atomic Energy Commission of Syria, Aalam Al-Zarra *92*, 99.

TRIFONOV, V.G., TRUBIKHIN, V.M., ADZHAMYAN, Z.H., DZHALLAD, S., EL'KHAIR, Y.U., and AYED, K.H. (1991), *Levant fault zone in northwest Syria*, Geotectonics *25*(2), 145–154.

ZOHDY, A.A.R. (1989), *A New Method for the Automatic Interpretation of Schlumberger and Wenner Sounding Curves*, Geophysics *54*, 245–253.

ZOHDY, A.A.R. and BISDORF, R.J. (1989), *Schlumberger Sounding Data Processing and Interpretation Program*, U. S. Geological Survey, Denver.

(Received July 21, 2008, revised May 17, 2009, accepted July 3, 2009, Published online November 27, 2009)